Supporting Information

Dickson et al. 10.1073/pnas.1218247109

SI Materials and Methods

We discuss further methodological considerations on use of the D1-secretory granule probe. In-cell use of this probe involves measurement of three fluorescence values: corrected fluorescence of cyan fluorescent protein $(CFP)_C$ and YFP_C for Förster resonance energy transfer (FRET) and citrine emission (YFP_Y) for pH at each time point, followed by application of an alkaline ammonium solution at the end of the experiment. With an apparatus capable of exciting at two wavelengths and measuring at two wavelengths, these measurements are straightforwardly accomplished in a few hundred milliseconds per point. The continuous pH measurement opens an opportunity to explore little-studied possible physiological pH signals. At high resolution, the YFP_Y brightness signal could, in principle, exhibit small decreases during occasional exocytosis of granules and loss of probe; however, exocytosis rarely involves more than a minute fraction of stored secretory granules (SGs), and we saw no decrement of YFP_Y with the KCl stimulus.

We developed a protocol to calibrate the D1-SG and D1-endoplasmic reticulum (ER) FRET ratio for Ca^{2+} and pH. The calibration relies on the structural identity of the calcium-sensing portion of these probes. The absolute Ca^{2+} values should be interpreted with caution, given their reliance on difficult calibrations. Compared with the similar D1-ER probe, the D1-SG probe requires more care to use because the expressed probe is not as bright. The fluorescence is very likely lower because, as we show, the acidity of SGs partially quenches the YFP and CFP, reducing the quantum yield, and because the SG compartment may have less volume or may traffic the probe less well than the ER in PC12 cells, reducing the total number of displayed molecules. A dimmer signal means that more attention must be paid to keeping a low and correct background. For example, we found that background is best measured at the end of the experiment rather than the beginning because the significant autofluorescence of glass bleaches quickly to a lower level after repeated exposure to exciting light. A correction that includes autofluorescence of an untransfected cell would be desirable. Again, the autofluorescence (mostly NADPH between 400 and 500 nm) bleaches and varies with the metabolic state of the cell. It would be desirable to use fluorescent probes of higher quantum efficiency, lower pK_a, and longer wavelength emission to alleviate some of these problems. With these difficulties, we find, for example, that the absolute SG Ca^{2+} values reported in the experiments are more variable than the ER Ca^{2+} values obtained with D1-ER-cameleon. Compared with D1-ER, the D1-SG probe also requires a more elaborate calibration over a range of pH and Ca^{2+}, taking care that the calibration solutions equilibrate with the ER, where the calibrating probe is expressed.

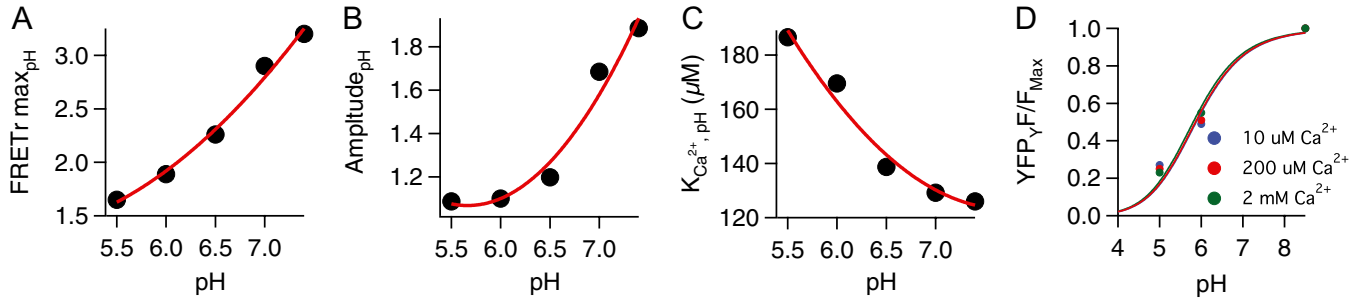

Fig. S1. pH dependence of parameters of the calibration equation. Symbols are pH dependence of the calibration parameters $FRET_{max,pH}$ (*A*), $Ampl_{pH}$ (*B*), and $K_{Ca,pH}$ (*C*) for Eq. **1**, and smooth curves are second-order polynomials (quadratic curves, Eq. **2**) fitted to them. (*D*) Titration of citrine by NH_4Cl is independent of Ca^{2+} concentration.

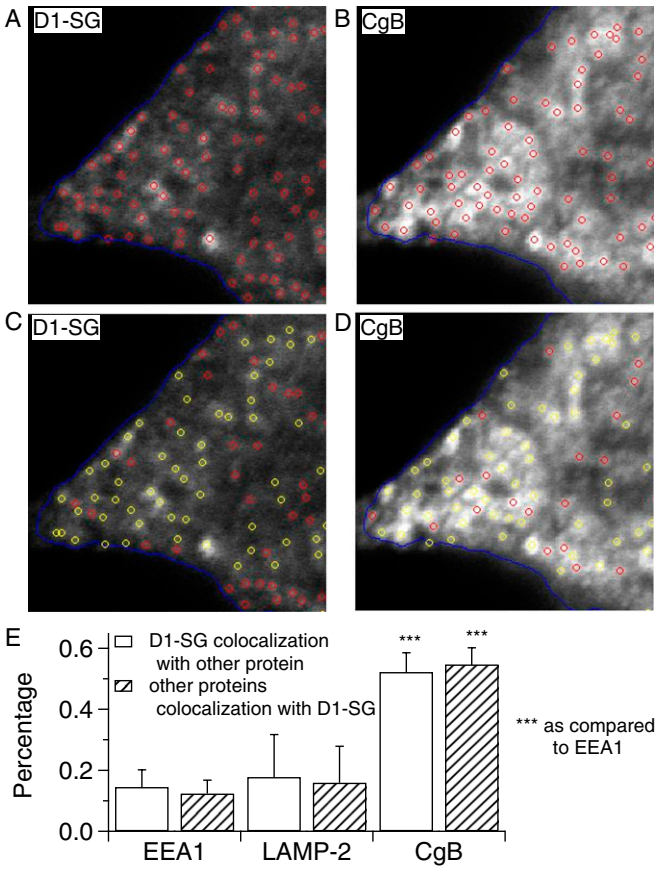

Fig. S2. Analysis of colocalization of granular objects shows that the majority of D1-SG localizes with SGs. This unique type of analysis, detailed in *Materials and Methods*, compares distances between multipixel puncta ("granular objects") of one protein and multipixel puncta of another with the distribution expected by chance. It is insensitive to the relative intensities of the probe and organelle markers. PC12 cells were transfected with D1-SG (green channel), and they were fixed and stained with a primary antibody against the desired organelle marker (red channel) 72 h later. We compare D1-SG with a marker for SGs, chromogranin B (CgB), in *A*–*D*. (*A*) D1-SG channel. Confocal image of a cell expressing D1-SG cameleon. Red circles mark the centers of the identified D1-SG–positive objects. (*B*) CgB channel. Confocal image from the same cell stained with CgB. Red circles mark the centers of identified CgB-positive objects. (*C*) D1-SG channel again. Yellow circles mark D1-SG–positive objects that fall within the criterion distance of CgB-positive objects (i.e., are colocalized). The remaining D1-SG–positive objects are still marked with red circles (not colocalized). From here, we can calculate the percentage of D1-SG–positive puncta that are colocalized. (*D*) CgB channel again. Here, the yellow circles mark CgB-positive objects that fall within the criterion distance of D1-SG–positive objects (colocalized). (*E*) Summary of the percentage of colocalized objects of different organelle markers (EEA1, early endosome antigen 1; LAMP-2, lysosome-associated membrane protein 2) in the total number of D1-SG objects in the D1-SG channel (open bars) and vice versa (hatched bars). The majority of D1-SG–positive objects are colocalized to SGs, and, reciprocally, the majority of CgB-positive objects have colocalized to D1-SG. There is some overlap between D1-SG and EEA1 and LAMP-2, but this is significantly smaller than CgB.

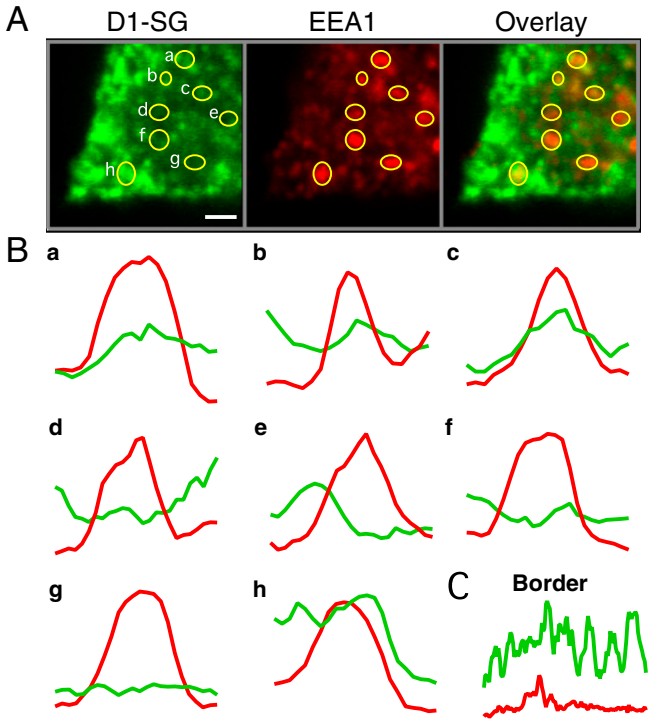

Fig. S3. Entry of the D1-SG probe into the endosomal pathway is minimal. Because SGs in PC12 cells spend time at the plasma membrane as they undergo exocytosis and recovery, it is likely that some D1-SG fluorescence would overlap with an early endosomal marker near the plasma membrane during the formation of the early endosomes. To determine whether D1-SG enters the endosomal pathway, we compared the distribution of early endosomal antigen 1 (EEA1) and D1-SG in PC12 cells. (*A*) Representative confocal images from cells expressing D1-SG cameleon (green, *Left*) or endosomal marker EEA1 (red, *Center*) and overlay. After they form, early endosomes move into the cytoplasm, where they undergo homotypic fusion (1, 2). The resulting endosomal compartment is visible in the cell interior as granule-sized puncta (Fig. 2). The D1-SG fluorescence is largely adjacent to the plasma membrane, whereas the largest and brightest EEA1-positive structures lie farther from the plasma membrane. Regions of interest (ROIs) marked by letters correspond to EEA1-positive structures. D1-SG and EEA1 overlap only infrequently. (*B*) Intensity scans of the D1-SG and EEA1 signals across the EEA1-positive structures are lettered as in *A*. ROI domains c and h are rare instances in which the two signals overlap. In the other cases, the D1-SG signal intensity shows little localization with the EEA1 signal. (*C*) Line scan along the length of the plasma membrane shows that there is some colocalization between the two proteins; however, the signal intensities and patterns of distribution are distinct. (Scale bar: 1 μm.)

1. Diaz R, Mayorga LS, Mayorga LE, Stahl P (1989) In vitro clustering and multiple fusion among macrophage endosomes. *J Biol Chem* 264(22):13171–13180.
2. Gorvel JP, Chavrier P, Zerial M, Gruenberg J (1991) rab5 controls early endosome fusion in vitro. *Cell* 64(5):915–925.

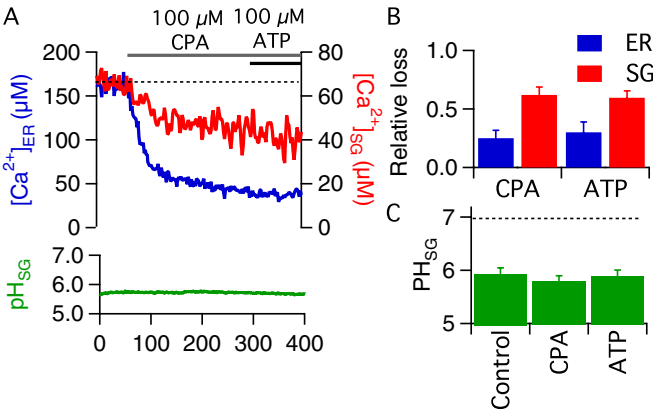

Fig. S4. Sarcoplasmic/endoplasmic reticulum Ca^{2+} ATPase (SERCA)-pump inhibitors reduce both $[Ca^{2+}]_{ER}$ and $[Ca^{2+}]_{SG}$. (*A*) Inhibiting the ER Ca^{2+}-ATPase with 100 μM cyclopiazonic acid (CPA) immediately initiated a decrease in $[Ca^{2+}]_{ER}$ (blue trace); further addition of ATP had no effect, confirming that ER stores are depleted. Similarly, 100 μM CPA caused a proportionally smaller decrease in $[Ca^{2+}]_{SG}$, with additional ATP application again having little effect. Changes in $[Ca^{2+}]_{ER}$ and $[Ca^{2+}]_{SG}$ were not accompanied by changes in SG pH (green line) . (*B* and *C*) Summary of calcium and pH in the ER and SG in response to CPA or ATP (n = 8).

Table S1. Summary of published granular free-Ca^{2+} measurements

Granule type	Species	Ca^{2+} probe	Resting [Ca^{2+}], μM	Granular response to IP_3	Granular response to KCl	Source
Chromaffin granules*	Cow	Ca^{2+} electrode†	N.D.	Ca^{2+} release‡	N.D.	(1)
Pancreatic zymogen granules*	Mouse	Mag-fura red	10–60	Ca^{2+} release‡	N.D.	(2)
Pancreatic zymogen granules*	Rat	Fura-2†	N.D.	No response‡	N.D.	(3)
Mucin granules*	Rabbit	Rhod-2/calcium orange-5N	20–35	Ca^{2+} oscillations‡,§	N.D.	(4)
MIN-6 β-cell granules	Mouse	VAMP-aequorin¶	~50	No response‡	N.D.	(5)
Mast cell granules*	Mouse	Ca^{2+} orange-5N	15–30	Ca^{2+} oscillations‡	N.D.	(6, 7)
PC12 granules	Rat	hCgA-aequorin¶	1–2¶	Ca^{2+} uptake§	Ca^{2+} uptake	(8)
PC12 granules	Rat	VAMP-aequorin¶	30–50	No response/Ca^{2+} release§,‖	Ca^{2+} release	(9)
PC12 granules	Rat	VAMP-aequorin¶	25–60	Ca^{2+} release‡	Ca^{2+} release	(10)
INS-1 cell insulin granules	Rat	VAMP-aequorin¶	20–40	Ca^{2+} release‡	Ca^{2+} uptake	(10)
PC12 granules	Rat	D1-SG	~70	No response§	Ca^{2+} uptake/release	This study

hCgA, human Chromogranin A; IP_3, inositol triphosphate; N.D., not done; tPA, tissue plasminogen activator; VAMP, vesicle associated membrane protein.
*Measurements were taken on preparations of isolated granules.
†Measurements were taken only outside of granules.
‡These studies applied IP_3 directly to membrane preparations and/or permeabilized cells.
§These studies applied ATP to the exterior of cells.
¶Aequorin construct used by Mitchell et al. (5), Moreno et al. (9), and SantoDomingo et al. (10) was a low-affinity mutant. That used by Mahapatra et al. (8) was the inappropriate high-affinity native aequorin; thus, we must dismiss their results.
‖Moreno et al. (9) saw Ca^{2+} release from PC12 granules after treatment with ATP but did not see release when they applied IP_3 to permeabilized cells.

1. Yoo SH, Albanesi JP (1990) Inositol 1,4,5-trisphosphate-triggered Ca^{2+} release from bovine adrenal medullary secretory vesicles. *J Biol Chem* 265(23):13446–13448.
2. Gerasimenko OV, Gerasimenko JV, Petersen OH, Tepikin AV (1996) Short pulses of acetylcholine stimulation induce cytosolic Ca^{2+} signals that are excluded from the nuclear region in pancreatic acinar cells. *Pflugers Arch* 432(6):1055–1061.
3. Yule DI, Ernst SA, Ohnishi H, Wojcikiewicz RJ (1997) Evidence that zymogen granules are not a physiologically relevant calcium pool. Defining the distribution of inositol 1,4,5-trisphosphate receptors in pancreatic acinar cells. *J Biol Chem* 272(14):9093–9098.
4. Nguyen T, Chin WC, Verdugo P (1998) Role of Ca^{2+}/K^{+} ion exchange in intracellular storage and release of Ca^{2+}. *Nature* 395(6705):908–912.
5. Mitchell KJ, et al. (2001) Dense core secretory vesicles revealed as a dynamic $Ca^{(2+)}$ store in neuroendocrine cells with a vesicle-associated membrane protein aequorin chimaera. *J Cell Biol* 155(1):41–51.
6. Quesada I, Chin WC, Steed J, Campos-Bedolla P, Verdugo P (2001) Mouse mast cell secretory granules can function as intracellular ionic oscillators. *Biophys J* 80(5):2133–2139.
7. Quesada I, Chin WC, Verdugo P (2003) ATP-independent luminal oscillations and release of Ca^{2+} and H^{+} from mast cell secretory granules: Implications for signal transduction. *Biophys J* 85(2):963–970.
8. Mahapatra, et al. (2004) A dynamic pool of calcium in catecholamine storage vesicles. Exploration in living cells by a novel vesicle-targeted chromogranin A-aequorin chimeric photoprotein. *J Biol Chem* 279(49):51107–51121.
9. Moreno A, et al. (2005) Calcium dynamics in catecholamine-containing secretory vesicles. *Cell Calcium* 37(6):555–564.
10. SantoDomingo J, et al. (2010) Ca2+ dynamics in the secretory vesicles of neurosecretory PC12 and INS1 cells. *Cell Mol Neurobiol* 30(8):1267–1274.